PPPL-2195

UC20-A

130
3-26-85 QS (2)

DR-C 792-3

I-20167

PPPL-2195

A HELICAL AXIS STELLARATOR EQUILIBRIUM MODEL

By

A.E. Koniges and J.L. Johnson

FEBRUARY 1985

PLASMA
PHYSICS
LABORATORY

PRINCETON UNIVERSITY

PRINCETON, NEW JERSEY

DISTRIBUTION OF THIS DOCUMENT IS UNLIMITED

PREPARED FOR THE U.S. DEPARTMENT OF ENERGY,
UNDER CONTRACT DE-AC02-76-CHO-3073.

DISCLAIMER

This report was prepared as an account of work sponsored by an agency of the United States Government. Neither the United States Government nor any agency thereof, nor any of their employees, makes any warranty, express or implied, or assumes any legal liability or responsibility for the accuracy, completeness, or usefulness of any information, apparatus, product, or process disclosed, or represents that its use would not infringe privately owned rights. Reference herein to any specific commercial product, process, or service by trade name, trademark, manufacturer, or otherwise does not necessarily constitute or imply its endorsement, recommendation, or favoring by the United States Government or any agency thereof. The views and opinions of authors expressed herein do not necessarily state or reflect those of the United States Government or any agency thereof.

PPPL--2195

DE85 008716

A Helical Axis Stellarator Equilibrium Model

A. E. Koniges[1]
Plasma Physics Laboratory and Program in Applied Mathematics
Princeton University, Princeton, NJ 08544
J. L. Johnson[2]
Plasma Physics Laboratory
Princeton University, Princeton, NJ 08544

An asymptotic model is developed to study MHD equilibria in toroidal systems with a helical magnetic axis. Using a characteristic coordinate system based on the vacuum field lines, the equilibrium problem is reduced to a two-dimensional generalized partial differential equation of the Grad-Shafranov type. A stellarator-expansion free-boundary equilibrium code is modified to solve the helical-axis equations. The expansion model is used to predict the equilibrium properties of Asperators NP-3 and NP-4. Numerically determined flux surfaces, magnetic well, transform, and shear are presented. The equilibria show a toroidal Shafranov shift.

---

[1]present address: Magnetic Fusion Energy Computer Center, Lawerence Livermore Laboratory, Livermore, California 94550

[2]On loan from Westinghouse Research and Development Center

MASTER

DISTRIBUTION OF THIS DOCUMENT IS UNLIMITED

I. Introduction

The concept of a toroidal stellarator with a nonplanar magnetic axis originated early in the fusion program.[1,2] The recent favorable outlook for the stellarator approach[3] has led to the exploration of new helical-axis configurations[4] which offer hopes for high-β confinement. To better understand the confinement properties of such devices, methods for analyzing configurations with nonplanar axes must be developed.

The complex topology of stellarator geometries makes theoretical MHD equilibrium analysis complicated. Since there is no ignorable coordinate, it is not possible to derive an exact Grad-Shafranov-type equation for the equilibrium.[5] Numerical equilibrium computation using three-dimensional computer codes has been successful for both planar and nonplanar devices.[6] However, three-dimensional calculations are limited to relatively coarse mesh size by the speed and memory of present computers, and in their ability to compute free-boundary equilibria. Approximate methods based on an expansion about a prescribed magnetic axis[7,8,9] have been used for the analysis of nonplanar toroidal systems. These methods are limited by difficulties in the incorporation of boundary conditions and by restrictions on the functional form of the assumed current and pressure profiles. There has been considerable success in using appropriate asymptotic expansions to reduce both the equilibrium and stability problems to simpler ones in two dimensions where a generalized partial differential equation of the Grad-Shafranov type can be obtained. For the conventional (planar axis) stellarator, the stellarator expansion of Greene and Johnson[10] and its numerical implemention for solving free-boundary equilibria[11] is currently a valuable tool

for design of devices and interpretation of experimental results. However, the assumptions made in the standard expansion yield a lowest-order configuration which has axial symmetry, and limit its applicability to systems with nearly planar axes.

In this paper, we develop an asymptotic model for MHD equilibria of systems with a helical magnetic axis of large radius. We interpret the nonplanar behavior of the magnetic axis as being associated with an $\ell = 1$ stellarator field, and use an ordering which is basically an extension of the standard stellarator expansion.[10] The major modification is that the wavelength of the primary helical field is treated as large with respect to the plasma radius, whereas in the standard stellarator expansion, these quantities are of the same order. Following the introduction of two length scales in the toroidal direction, we transform to a characteristic coordinate system based on the lowest-order vacuum field lines, which follow a helical path. This enables us to implement the standard asymptotic procedure[12] of integrating the lowest-order equations and removing secular terms in higher order analytically. The equilibrium problem is reduced to the solution of a two-dimensional Grad-Shafranov-like equation. The problem is solved using numerical techniques developed for the standard stellarator expansion. In this paper, we study the equilibrium properties of a large-aspect-ratio, low-β, $\ell = 1$ stellarator, although the formalism can be extended to treat systems with more complicated fields.

We present the governing equations in Sec. II. In Sec. III, we discuss the geometry, the vacuum fields, and the asymptotic ordering. In Sec. IV, we introduce the characteristic coordinates and reduce the problem to a two-dimensional

formulation. Some equilibrium quantities are calculated in Sec. V. The boundary conditions are presented in Sec. VI. Applications of the model are given in Sec. VII.

II. Basic Equations

The static equilibrium configuration is described by the MHD equations,

$$\nabla P = \mathbf{J} \times \mathbf{B}, \tag{1}$$

$$\nabla \cdot \mathbf{B} = 0, \tag{2}$$

$$\nabla \times \mathbf{B} = \mathbf{J}. \tag{3}$$

It is convenient to cast these equations into the form of two magnetic differential equations and a vector Poisson equation. We assume the configuration has nested topologically toroidal magnetic surfaces which we label as the level surfaces of a function Ψ, and prescribe a functional dependence for the scalar pressure, $P = P(\Psi)$. (In Section V, Ψ is chosen to be proportional to the poloidal flux.) Then Eq. (1) yields

$$\mathbf{B} \cdot \nabla \Psi = 0. \tag{4}$$

We write the total magnetic field as

$$\mathbf{B} = \mathbf{B}_{\rm vac} + \mathbf{B}^{\alpha} + \mathbf{B}^{\beta},$$

where $\mathbf{B}_{\rm vac}$ is the vacuum field, and $\mathbf{B}^{\alpha}$ and $\mathbf{B}^{\beta}$ are the fields induced by currents parallel and perpendicular to the field, respectively. Following standard

procedure, we split the current density into perpendicular and parallel components,

$$\mathbf{J} = \mathbf{J}_\perp + \sigma \mathbf{B},$$

where, from Eq. (1),

$$\mathbf{J}_\perp = \frac{\mathbf{B} \times \nabla P}{\mathbf{B}^2}$$

and

$$\sigma \equiv \frac{\mathbf{J} \cdot \mathbf{B}}{\mathbf{B}^2}.$$

The fields induced by these currents can be divided into components $\mathbf{B}^\beta$ and $\mathbf{B}^\sigma$, with

$$\nabla \times \mathbf{B}^\beta = \mathbf{J}_\perp$$

and

$$\nabla \times \mathbf{B}^\sigma = \sigma \mathbf{B}.$$

It is convenient to write $\mathbf{B}^\sigma$ in terms of a vector potential,

$$\mathbf{B}^\sigma = \nabla \times \mathbf{A}^\sigma,$$

and, choosing the gauge with $\nabla \cdot \mathbf{A}^\sigma = 0$, we have

$$\nabla^2 \mathbf{A}^\sigma = \sigma \mathbf{B}. \tag{5}$$

A magnetic differential equation for σ,

$$\mathbf{B} \cdot \nabla \sigma = \frac{\mathbf{B} \times \nabla P \cdot \nabla B^2}{B^4}, \tag{6}$$

is obtained from the condition that $\mathbf{J}$ be divergence-free.

Equations (4), (5), and (6) will be used in conjunction with the expansion developed in the next section to form a generalized partial differential equation for the lowest-order equilibrium configuration.

III. Vacuum Field and Expansion Ordering

The model geometry is a tube with a helical axis; the helical axis is inscribed in a cylinder which is bent into a torus with a large radius of curvature. The radius of the cylinder defines the helical radius. The helix is periodic over a length $2\pi/h$. The vacuum field, $\mathbf{B}_{\mathrm{vac}}$, is the superposition of a toroidal field, $\mathbf{B}_0$, which is constant to lowest order, and an $\ell = 1$ helical stellarator field, $\mathbf{B}_{\mathrm{H}}$. The toroidal curvature is introduced by solving for the vacuum field potential in a pseudo-toroidal coordinate system. This orthogonal coordinate system is defined by giving the metric

$$dl^2 = dr^2 + r^2 d\omega^2 + \left(1 + \frac{r}{R}\cos\omega\right)^2 dz^2, \tag{7}$$

where (r, ω, z) is a local cylindrical system centered on the toroidal axis, and R is the major radius of the torus. The toroidal field $\mathbf{B}_0$ is written in terms of a scalar potential proportional to z, and curvature terms associated with this field enter through expansion of the gradient operator in powers of the curvature. The scalar potential for the helical field $\mathbf{B}_{\mathrm{H}}$ is a solution of Laplace's equation in pseudo-toroidal coordinates, which is helically symmetric to lowest order.

The assumptions motivating the ordering are that the magnitude of the helical field is small with respect to the toroidal field and that the wavelength of the helical field is sufficiently long that the distortion of the magnetic axis from being straight (i.e., thehelical radius) is of the same order as the plasma radius. This leads to an ordering in which the plasma radius is small with respect to the helical wavelength, which in turn is small with respect to the toroidal circumference. To incorporate these into the framework of a stellarator

expansion, we introduce two length scales in z, a rapid variation that is periodic over one helical period denoted by t, and a slow variation all the way around the torus denoted by ς. We assume that *all* physical scalars are periodic functions of t as well as ς. We introduce dimensionless variables

$$x = \frac{r}{a}\cos\omega, \quad y = \frac{r}{a}\sin\omega, \quad t = hz, \quad \varsigma = \frac{z}{a}, \tag{8}$$

where a is the minor radius of the plasma. Then, standard multiple-scale analysis gives

$$a\frac{\partial}{\partial z} = \frac{\partial}{\partial \varsigma} + \gamma\frac{\partial}{\partial t} + \cdots,$$

where $\gamma \equiv ha \ll 1$.

In what follows, we work in a set of units with lengths normalized to the plasma radius a and magnetic fields normalized to the toroidal field strength $|\mathbf{B}_0|$. We define a basic expansion parameter δ, measuring the relative strength of the helical field with respect to the toroidal field. The geometric parameters are ordered in terms of δ as

$$\delta \sim \gamma \sim \epsilon^{\frac{1}{2}},$$

where $\delta \equiv |\mathbf{B}_H|/|\mathbf{B}_0|$, and $\epsilon \equiv a/R$ is the inverse aspect ratio. Then, the total vacuum field $\mathbf{B}_{\rm vac}$ is expressed in terms of a scalar potential, $\mathbf{B}_{\rm vac} = \nabla\Phi$, with

$$\begin{aligned}\Phi = \varsigma + \gamma\Delta(y\cos t - x\sin t) + \frac{\gamma^3\Delta}{8}(x^2+y^2)(y\cos t - x\sin t) \\ + \frac{\gamma\epsilon\Delta\rho^2}{4}\sin t + O(\delta^4),\end{aligned} \tag{9}$$

where $\Delta \equiv \delta/\gamma = O(1)$. The $\gamma\epsilon\Delta$ term arises from the coupling between helicity and toroidicity in solving Laplace's equation for the helical field. The ordering of γ with respect to δ is chosen to ensure that the cylindrical radius of the helix

be of the same order as the plasma radius, and the ordering of ϵ is chosen so that all three parameters enter the expression for the lowest-order flux surfaces.

The helical nature of the magnetic field lines is best observed by considering the field-line equations,

$$\frac{dx}{B_x} = \frac{dy}{B_y} = \frac{dt(1+\epsilon x)}{\gamma B_z}.$$

To lowest order, we have

$$\frac{dx}{dt} = -\frac{\delta}{\gamma}\sin t, \qquad x = x_0 - \frac{\delta}{\gamma} + \frac{\delta}{\gamma}\cos t,$$

$$\frac{dy}{dt} = \frac{\delta}{\gamma}\cos t, \qquad y = y_0 + \frac{\delta}{\gamma}\sin t,$$

where the constants x_0 and y_0 are the intercepts of the field lines with the $t = 0$ surface. (In the standard stellarator expansion where $\gamma \sim 1$, the field lines follow a circular path around the torus to lowest order.) Carrying the integration of these equations for the vacuum field lines to higher order shows that the rotational transform is $\iota = \delta^2/2$ per helical period. (Our definition of ι differs from that of Greene and Johnson[10] by a factor of 2π.) Since the total number of helical periods is γ/ϵ, the transform over a complete circuit of the torus is of order δ.

The effects of plasma pressure and current on the equilibrium enter through the fields $\mathbf{B}^\delta$ and $\mathbf{B}^\sigma$ introduced in the previous section. We choose the ordering of the pressure so that it affects the lowest-order magnetic surfaces. It will be shown in the next section that, given the ordering of the vacuum field parameters δ, γ, and ϵ, the third-order components of $\mathbf{B}_\perp$ affect the determination of Ψ to lowest order through Eq. (4). This fixes the size of $\mathbf{B}^\sigma$, and we can determine

the order of $\mathbf{B}^\beta$ from Eq. (6). Thus we take

$$\frac{B^\sigma}{B_0} \sim \delta^3, \qquad \frac{B^\beta}{B_0} \sim \delta^4.$$

This is a maximal balance ordering in the sense that all the ordered physical quantities enter into the determination of the lowest-order magnetic surfaces.

IV. Integration

In this section, we use the asymptotic expansion to simplify and integrate the equations introduced in Sec. II. Since $\mathbf{B}$ is a constant field in the toroidal direction in lowest order, we can simplify the lowest-order vector potential to one component $\mathbf{A}^\sigma = A(x,y,t)\hat{\mathbf{z}} + \cdots$. (Here, $\hat{\mathbf{z}}$ is the unit vector in the toroidal direction.) Then Eq. (5) reduces to an inhomogeneous scalar equation

$$\nabla_\perp^2 A = \sigma, \tag{10}$$

where $\nabla_\perp^2 \equiv \partial^2/\partial x^2 + \partial^2/\partial y^2$.

The two magnetic differential equations (4) and (6) can be integrated order by order. An efficacious transformation to a coordinate system based on the characteristics of the operator $\mathbf{B}\cdot\nabla$ enables us to formulate the equilibrium problem in two dimensions.

We start with Eq. (4) for the magnetic surfaces and expand

$$\Psi(x,y,t,\varsigma) = \Psi^{(0)} + \Psi^{(1)} + \ldots, \tag{11}$$

where superscripts denote order with respect to δ. The equation in lowest order is

$$\frac{\partial \Psi^{(0)}}{\partial \varsigma} = 0,$$

and periodicity requires that

$$\Psi^{(0)} = \Psi^{(0)}(x, y, t),$$

which means $\Psi^{(0)}$ is allowed to vary in the toroidal direction only over the short (helical) period. It can be shown that all ς *dependence* is similarly eliminated order by order. The argument follows from Kruskal's *theorem of phase independence.*[13]

In the next order,

$$L\left[\Psi^{(0)}\right] \equiv \frac{\partial \Psi^{(0)}}{\partial t} - \Delta \sin t \frac{\partial \Psi^{(0)}}{\partial x} + \Delta \cos t \frac{\partial \Psi^{(0)}}{\partial y} = 0. \tag{12}$$

This first-order linear equation is conveniently solved by integrating the characteristic equations,

$$\frac{dt}{1} = \frac{-dx}{\Delta \sin t} = \frac{dy}{\Delta \cos t}; \qquad d\Psi^{(0)} = 0.$$

Solving simultaneously yields the general solution,

$$\Psi^{(0)} = \Psi^{(0)}(C_1, C_2), \tag{13}$$

where

$$C_1 \equiv x - \Delta \cos t, \qquad C_2 \equiv y - \Delta \sin t. \tag{14}$$

Similarly, in second order, we find

$$\Psi^{(1)} = \Psi^{(1)}(C_1, C_2).$$

The functional form of $\Psi^{(0)}$ is determined by the third-order equation,

$$L\left[\Psi^{(2)}\right] = -\frac{B_x^{(3)}}{\gamma}\frac{\partial \Psi^{(0)}}{\partial x} - \frac{B_y^{(3)}}{\gamma}\frac{\partial \Psi^{(0)}}{\partial y} + \left[\gamma\delta(y \sin t + x \cos t) + 2\epsilon x\right]\frac{\partial \Psi^{(0)}}{\partial t},$$

where $B_x^{(3)}$ and $B_y^{(3)}$ are the third-order components of the full magnetic field. The general solution for $\Psi^{(2)}$ can be obtained by transforming to a characteristic coordinate system $(C_1, C_2, \hat{t})$, where C_1 and C_2 are given in Eq. (14) and $\hat{t} = t$. Note that in this coordinate system, the operator $L\left[\Psi^{(2)}\right]$ of Eq. (12) becomes $\partial\Psi^{(2)}/\partial\hat{t}$. The condition that $\Psi^{(2)}$ be periodic over a helical period,

$$\int_0^{2\pi} \frac{\partial \Psi^{(2)}}{\partial \hat{t}}\, d\hat{t} = 0,$$

reduces to a first-order partial differential equation which determines the functional form of $\Psi^{(0)}$, namely

$$\frac{\partial \Psi^{(0)}}{\partial C_1}\left[\frac{\gamma^3\Delta^2}{2}C_2 + \frac{1}{\gamma}\frac{\partial \bar{A}}{\partial C_2}\right] - \frac{\partial \Psi^{(0)}}{\partial C_2}\left[\frac{\gamma^2\Delta^2}{2}C_1 + \frac{5\epsilon\Delta^2}{\gamma} + \frac{1}{\gamma}\frac{\partial \bar{A}}{\partial C_1}\right] = 0. \quad (15)$$

Here, barred quantities are averages over the helical period,

$$\bar{A}(C_1, C_2) \equiv \frac{1}{2\pi}\int_0^{2\pi} A(C_1, C_2, \hat{t})\, d\hat{t}.$$

Integration of Eq. (15) shows that $\Psi^{(0)}$ is a function of

$$C_1^2 + C_2^2 + \frac{5\epsilon}{\gamma^2}C_1 + \frac{4\bar{A}}{\delta^2\gamma}.$$

We choose it to be a linear function in order that $\Psi^{(0)}$ be proportional to the poloidal flux which is calculated in the next section. In particular, we write

$$\Psi^{(0)} = C_1^2 + C_2^2 + \frac{5\epsilon}{\gamma^2}C_1 + d^2 + \frac{4\bar{A}}{\delta^2\gamma}, \quad (16)$$

where

$$d \equiv \frac{5\epsilon}{2\gamma^2}.$$

There is no loss of generality in choosing $\Psi^{(0)}$ to be proportional to the poloidal flux. This is just the freedom to label surfaces in a particular way.

Integration of Eq. (6), the magnetic differential equation for σ, is similarly expedited by working in the characteristic coordinate system, since the operator $\mathbf{B}\cdot\nabla$ is the same in both cases. With $\nabla P(\Psi) = P'(\Psi^{(0)})\nabla\Psi^{(0)} + \ldots$, Eq. (6) becomes

$$\mathbf{B}\cdot\nabla\sigma = P'(\Psi^{(0)})\left[(2\gamma\delta\cos t + 2\epsilon)\frac{\partial\Psi^{(0)}}{\partial C_2} + 2\gamma\delta\sin t\frac{\partial\Psi^{(0)}}{\partial C_1} + O(\delta^3)\right].$$

Proceeding as before, we find in fourth order

$$\sigma^{(3)} = \sigma^{(3)}(C_1, C_2).$$

Again, the functional form of σ is determined by the periodicity constraint in higher order,

$$\int_0^{2\pi}\frac{\partial\sigma^{(3)}}{\partial\hat{t}}\,d\hat{t} = 0,$$

which yields

$$\frac{\partial\sigma^{(3)}}{\partial C_1}\left[\frac{\gamma^2\Delta^2}{2}C_2 + \frac{1}{\gamma}\frac{\partial\tilde{A}}{\partial C_2}\right] - \frac{\partial\sigma^{(3)}}{\partial C_2}\left[\frac{\gamma^2\Delta^2}{2}C_1 + \frac{5\epsilon\Delta^2}{\gamma} + \frac{1}{\gamma}\frac{\partial\tilde{A}}{\partial C_1}\right]$$

$$+ \frac{2\epsilon}{\gamma}P'(\Psi^{(0)})\frac{\partial\Psi^{(0)}}{\partial C_2} = 0.$$

Integration gives

$$\sigma^{(3)} = \frac{-8\epsilon}{\gamma\delta^2}P'(\Psi^{(0)})C_1 + F(\Psi^{(0)}), \tag{17}$$

where F is an arbitrary function. The freedom to specify F allows us to calculate equilibria with zero net current.

Finally, we consider Eq. (10) for A. Since to lowest-order σ is a function of C_1 and C_2 only, we take $A = \tilde{A}$. We express Eq. (10) in the characteristic coordinate system as

$$\frac{\partial^2 A}{\partial C_1^2} + \frac{\partial^2 A}{\partial C_2^2} = \sigma^{(3)}(C_1, C_2). \tag{18}$$

The coupled set, Eqs. (16), (17), and (18), can be combined to yield a generalized partial differential equation of the Grad-Shafranov type, similar to that obtained using the standard stellarator expansion.[16] In Sec. VI, we specify the surface functions $P'(\Psi^{(0)})$ and $F(\Psi^{(2)})$ of Eq. (17) and discuss the boundary conditions for the system.

V. Equilibrium Quantities

The equilibrium configuration is characterized by the magnetic surface function Ψ, given to lowest order by Eq. (16). In the vacuum limit, we have circular flux surfaces with fixed radius $\Psi^{(0)\frac{1}{2}}$, centered on a helical magnetic axis given by $x = \Delta\cos t - d$, and $y = \Delta\sin t$, where (x, y, t) are the normalized pseudo-toroidal coordinates. Toroidal effects enter these lowest-order vacuum surfaces since the constant shift $d = 5\epsilon/2\gamma^2$ is proportional to the inverse aspect ratio. The effect of current in the plasma enters through the stream function $A(C_1, C_2)$.

It is convenient to calculate equilibrium quantities in a $(\rho, \theta, \hat{t})$ coordinate system with origin centered on the vacuum magnetic axis,

$$\rho = [(C_1 + d)^2 + C_2^2]^{\frac{1}{2}}, \quad \theta = \tan^{-1}[C_2/(C_1 + d)], \quad \hat{t} = t,$$

where C_1 and C_2 are defined in Eq. (14). Then, the angular coordinate function θ increases by 2π during one loop around the magnetic axis the short way, and the poloidal flux per helical period is[14]

$$\Psi_{\rm pol} = \frac{1}{2\pi}\int_V b^\theta \, d\tau.$$

Here, V is the volume enclosed by the surface in question, and the superscript

on b denotes a contravariant component of the field $\mathbf{B}$, namely

$$b^\theta = \frac{-\sin\theta}{\rho}\left[B_x - \Delta\cos\hat{t}\left(\frac{\gamma B_x}{1+\epsilon x}\right)\right] + \frac{\cos\theta}{\rho}\left[B_y + \Delta\sin\hat{t}\left(\frac{\gamma B_x}{1+\epsilon x}\right)\right] + O(\delta^5).$$

Also,

$$d\tau = \frac{(1+\epsilon x)}{\gamma}\rho\, d\rho\, d\theta\, d\hat{t}, \qquad x = \rho\cos\theta - \Delta\cos\hat{t} - d.$$

Evaluating the integral over $\hat{t}$ and doing some manipulating yields

$$\Psi_{\rm pol} = \int_0^{2\pi} d\theta \int_0^{\rho(\Psi^{(0)},\theta)} \frac{\delta^2}{4}\frac{\partial\Psi^{(0)}(\rho,\theta)}{\partial\rho}\, d\rho = \frac{\pi\delta^2}{2}\Psi^{(0)},$$

where we have retained terms through third order in δ.

The toroidal flux is given by[14]

$$\Psi_{\rm tor} = \frac{1}{2\pi}\int b^t\, d\tau$$

$$= \int_0^{2\pi} d\theta \int_0^{\rho(\Psi^{(0)},\theta)} (1 - \epsilon(\rho\cos\theta - d) - \gamma^2\Delta^2)\rho\, d\rho + O(\delta^3).$$

In lowest order where the toroidal field is constant, the toroidal flux is the cross-sectional area enclosed by a given flux surface $\Psi^{(0)}$. This can be written in a flux coordinate system as

$$\Psi_{\rm tor} = \int_0^{\Psi^{(0)}} d\Psi^{(0)} \int \frac{dl}{|\nabla\Psi|},$$

where $dl^2 = d\rho^2 + \rho^2 d\theta^2$. The rotational transform obtained in this manner,

$$\iota \equiv \frac{d\Psi_{\rm pol}}{d\Psi_{\rm tor}} = \pi\frac{\delta^2}{2}\left[\int \frac{dl}{|\nabla\Psi|}\right]^{-1},$$

agrees in the vacuum limit with the transform obtained by integrating the vacuum field-line equations,

$$\iota_{\rm vac} = \frac{\delta^2}{2}.$$

The volume enclosed by a given flux surface,

$$V = \frac{1}{\gamma}\int d\tau = \int_0^{2\pi} d\hat{\iota}\int_0^{2\pi} d\theta \int_0^{\rho(\Psi^{(0)},\theta)} \rho\, d\rho (1+\epsilon(\rho\cos\theta - d)) + O(\delta^4),$$

can be used to calculate the magnetic well, which provides a stability estimate. By adding and subtracting $b^t(1+\epsilon(\rho\cos\theta - d))$ from the integrand,[10] we can write V in terms of the toroidal flux and a flux surface integral;

$$V = \frac{2\pi}{\gamma}\Psi_{\rm tor} + \frac{1}{\gamma}\int d\Psi^{(0)} \int \frac{dl}{|\nabla\Psi|}\left[2\epsilon\left(\rho\cos\theta - d\right) + \gamma^2\Delta^2\right] + O(\delta^4).$$

This form is useful for computing the well $V''(\Psi_{\rm tor})$, where the prime denotes derivative with respect to the argument, since the potentially stabilizing integral term can be computed by numerically integrating terms of finite order. To the order of this calculation, $V''(\Psi_{\rm tor}) = 0$ in the vacuum limit. We note that due to the chosen ordering, this result does not contain a term associated with the diamagnetic currents that maintain the plasma pressure, as was the case in the standard stellarator expansion.[10]

VI. Boundary Conditions and Numerical Solutions

In this section, we pose two boundary-value problems for Eq. (18). The free-boundary problem is analogous to those solved by standard iterative stellarator equilibrium codes, and we have modified a version of PEST[11,15] to solve these helical-axis equations. The details of these modifications are given elsewhere.[16]

A. Free-Boundary Problem

Consider a plasma surrounded by a vacuum, so that $\nabla_\perp^2 A = 0$ in the vacuum and $\nabla_\perp^2 A = \sigma$ in the plasma. A free-boundary problem is formulated in

the following way.[11,15] Using an initial guess for σ and $\Psi^{(0)}$, we numerically determine the Dirichlet condition $A|_{\text{boundary}}$ of the computational domain by integrating the product of σ and the free-space Green's function $G(\mathbf{r}_B, |\mathbf{r}_P,)$ for the two-dimensional Laplacian operator,

$$G(\mathbf{r}_B|\mathbf{r}_P) = -2\log\left(\frac{|\mathbf{r}_B - \mathbf{r}_P|}{|\mathbf{r}_P|}\right),$$

over the plasma region. Here, $\mathbf{r}_B$ is a point on the boundary, and $\mathbf{r}_P$ is a point in the plasma. This is equivalent to the assumption that the plasma itself is the only current source, and that the influence of the current source drops to zero far from the plasma. We note that it is straightforward to modify the Green's function formulation to include the effects of external current sources.[10] Given $A|_{\text{boundary}}$, we invert Eq. (18) to find A, and calculate $\Psi^{(0)}$ from Eq. (16). This yields a new value for σ from Eq. (17) and the procedure is repeated until a self-consistent solution is obtained.

In general, two surface functions must be given in order to specify the equilibrium completely.[14] The pressure is prescribed by

$$P = P_0\left(\frac{{\Psi^{(0)}}_{\text{lim}} - \Psi^{(0)}}{{\Psi^{(0)}}_{\text{lim}} - {\Psi^{(0)}}_{\text{min}}}\right)^k, \tag{19}$$

where ${\Psi^{(0)}}_{\text{lim}}$ is the value at a limiter which defines the plasma boundary in the vacuum limit and ${\Psi^{(0)}}_{\text{min}}$ is the minimum value of $\Psi^{(0)}$ on the grid. A common choice is $k = 2$. The free function $F(\Psi^{(0)})$ in Eq. (17) is iteratively determined such that the pure stellarator condition is satisfied, i.e., no net toroidal current on each surface. Thus,

$$F(\Psi^{(0)}) = \frac{8\epsilon}{\gamma\delta^2} P'(\Psi^{(0)}) \int C_1 \frac{dl}{|\nabla\Psi^{(0)}|}\left[\int \frac{dl}{|\nabla\Psi^{(0)}|}\right]^{-1}.$$

We note that we can add to this an additional function of $\Psi^{(0)}$ in order to model equilibria with net toroidal current.

B. Fixed-Boundary Problem

The fixed-boundary problem is equivalent to surrounding the plasma with a perfectly conducting shell. (Often, the shape of the shell is chosen to coincide with a vacuum surface.) If the conducting shell's cross section is a circle in (C_1, C_2) space, it is possible to write the solution in closed form as an integral equation. Hence, we solve $\nabla_\perp^2 A = \sigma$ with $\Psi^{(0)} =$ constant at $\rho = 1$. The Green's function for this problem can be obtained by conformally mapping the relevant half-plane Green's function into the unit disk, yielding[17]

$$G(\rho,\theta|r,s) = \frac{1}{4\pi}\log\left[\frac{\rho^2 - 2\rho r\cos(\theta - s) + r^2}{1 - 2\rho r\cos(\theta - s) + \rho^2 r^2}\right] \qquad (\rho \le 1).$$

Then,

$$\Psi^{(0)}(\rho,\theta) = \int_{\text{disk}} r\,dr\,ds\left[4\left(1 + \frac{\sigma(\Psi^{(0)})}{\delta^2\gamma}\right)G(\rho,\theta|r,s)\right],$$

where we have used the relation,

$$\nabla^2\Psi^{(0)} = 4 + \frac{4}{\delta^2\gamma}\nabla^2 A.$$

Again, $P(\Psi^{(0)})$ is a specified function, and $F(\Psi^{(0)})$ can be determined iteratively to satisfy a condition on the net current.

VII. Applications

We use the helical-axis stellarator expansion to model two stellarators at Tohoku University,[18,19] Asperators NP-3 and NP-4. Each of these devices has

a helical magnetic axis which closes upon itself following one circuit in the toroidal direction. The primary magnetic field is produced by circular solenoids centered on a helical axis. This helical field should be adequately modeled using the $\ell = 1$ potential of the helical-axis stellarator expansion. Device parameters for NP-3 and NP-4, together with the appropriate parameters for the expansion, are given in Table I.[18,19]

The helical-axis stellarator expansion yields flux surfaces which are nested on a primarily helical axis. The toroidal dependence of the configuration is depicted in Fig. 1(a), which shows the surfaces at three different t-planes for the NP-3 device with an average beta $\langle\beta\rangle = 34\%$. The large cross marks the center of the pseudo-toroidal coordinates (x, y, t), i.e., the center of the $\ell = 1$ field. The model predicts a toroidal Shafranov shift, which introduces both shear and a magnetic well. The shear is evidenced in Fig. 1(b), since the rotational transform is not constant. Figure 1(c) shows the well, since $V'(\Psi_{tor})$ is a monotonically decreasing function. In the remainder of the plots, the magnetic flux surfaces are shown at a single value of t with the physical center of the plot coinciding with the vacuum-field magnetic axis. In plots of the equilibrium quantities, $D_1 = 0$ marks the vacuum-field magnetic axis.

The effects of changing plasma pressure on the NP-3 configuration are shown in Fig. 2. The vacuum-field magnetic surfaces are given in Fig. 2(a). The concentric circles are centered on the vacuum magnetic axis, which is shifted towards the curvature center of the torus a distance of $5\epsilon a_p/2\gamma^2 = 0.8$ cm with respect to the geometric center of the toroidal field coils. The effects of increasing the pressure are shown in Fig. 2(b) with $\langle\beta\rangle = 17\,\%$ and in Fig. 2(c)

with $\langle\beta\rangle = 50\,\%$.

The vacuum configuration for NP-4 is given in Fig. 3(a). The vacuum magnetic axis is shifted 2.4 cm with respect to the geometric center of the toroidal field coils. The effects of pressure on the configuration are shown in Fig. 3(b) with $\langle\beta\rangle = 17\,\%$ and Fig. 3(c) with $\langle\beta\rangle = 33\,\%$. As $\langle\beta\rangle$ increases, the entire plasma shifts away from the center of the torus and the Shafranov shift of the innermost surfaces is clearly seen. We note that the plasma can be recentered by applying an external vertical field.

In all the results presented up to this point, the exponent k in the pressure function Eq. (19) has been set equal to 2.0, corresponding to a parabolic distribution in Ψ. The effects of varying this exponent are shown in Fig. (4). Figure 4(a) gives ι and $V'(\Psi_{\rm tor})$ as functions of $\Psi_{\rm pol}$ for $k = 1.5$ and Fig. 4(b) shows these functions for $k = 3.0$. The average beta is 33% in both cases. The value of ι and V' on axis is the same for both values of k. For the steeper pressure profile, $k = 3.0$, V' decreases rapidly near the axis and then becomes flat near the plasma boundary. The shear in this case is strongest near the axis.

In summary, our vacuum configuration has circular flux surfaces which are rigidly shifted towards the center of the torus due to the toroidal curvature. The rotational transform is constant for the vacuum case, with the same value $\iota = 0.5$ obtained for both devices. Funato *et al.*[20] give some numerical and experimental results for the vacuum configuration of the NP-4 device. They find that the vacuum configuration formed by the circular solenoidal coils consists of nested circles with the magnetic axis shifted by about 1.6 cm from the geometric center of the coils towards the center of the torus. An electron beam method

is used to measure a mean rotational transform per helical period, $\iota = 0.7$,[20,21] which is approximately constant across the flux surfaces. Their results are in qualitative agreement with those given here.

The primary effect of pressure on the configuration is to induce a Shafranov shift, which produces a magnetic well and creates shear. At very high beta values, the entire plasma is shifted away from the center of the torus, and an external field is required to keep the plasma inside the vacuum vessel. The model predicts that the Asperator configurations are capable of achieving equilibrium beta values on the order of $\langle\beta\rangle = 50\,\%$. For a given beta value, the Shafranov shift is significantly less pronounced for NP-3 than for NP-4. Trubnikov and Dobryakov[22] investigated plasma equilibrium in a stellarator whose magnetic axis is a (helically wrapped) geodesic on a torus, and found that if the inverse aspect ratio $\epsilon \leq 0.1$, a substantial decrease in the shift is obtained when the number of helical periods is increased from 8 to 16. This agrees with our findings for NP-3 with 16 periods and NP-4 which has 8 helical periods.

VIII. Discussion and Conclusions

The primary focus of this work is on the development of an asymptotic technique for reducing the equilibrium problem for a helical-axis stellarator to a two-dimensional Grad-Shafranov-type equation. The motivation for seeking this reduction is to make use of the variety of analytic and numerical methods available for the analysis of two-dimensional MHD equilibria. These include efficient free-boundary equilibrium codes and a formalism for stability analysis using expansion techniques.[23] In the case of the conventional stellarator, the

inherently three-dimensional equilibrium problem can be expressed to lowest order as a two-dimensional problem that has axisymmetry, with toroidal effects provided by a self-consistent determination of the Pfirsch-Schlüter currents.[10] At first, it is not obvious that a similar simplification procedure can be developed for a helical-axis stellarator. The key to solving the helical-axis problem is the introduction of a coordinate system based on the characteristics of the lowest-order vacuum field lines. These characteristic coordinates assume the same role that the axisymmetric coordinates assume in the case of the conventional stellarator. We note that the results of this study connect smoothly to those obtained in the standard stellarator expansion.[10] Namely, the expression for the vacuum surface function Ψ in the asymptotic limits of small Δ in the helical-axis expansion and small γ in the standard expansion coincide when we retain both zeroth and first-order terms in the latter.

The helical-axis stellarator expansion provides a useful model of the Asperator NP-3 and NP-4 devices. The vacuum field predictions for the equilibrium properties are in qualitative agreement with other analyses. In this paper, we are able to estimate the effects of pressure on the equilibrium, while most previous studies concentrated on modeling the vacuum configurations. High-beta equilibria with significant shear and a magnetic well are predicted.

The ordering of the parameters chosen in this paper led to the result that the rotational transform over the torus is small, of order δ, rather than finite as in the standard stellarator expansion. Because of this, we had to order the pressure very small, $P \sim \delta^4$. An alternate way to model the configuration would have been to increase the major radius as we extend the length of the helical

period, which leads to the ordering

$$\delta^3 \sim \gamma^3 \sim \epsilon \sim \beta \sim \sigma \ll 1.$$

Then, the transform would be finite. The use of this alternate ordering would yield essentially the same results, with the exception that the toroidally inward displacement d of Eq. (13) would be absent. Based on previous studies,[23] we believe that this ordering is the approriate one for stability investigations.

This study has much in common with the work of Hender and Carreras[24] who also use a stellarator expansion to reduce the helical-axis stellarator equilibrium problem to two dimensions. Rather than modeling the helical fields explicitly by introducing an $\ell = 1$ potential, they use a numerically determined vacuum field and work in a vacuum flux coordinate system. They have shown that the calculation of the equilibrium properties can be carried further than was done in our work, by determining the effects of the helical Pfirsch-Schlüter currents as well as the toroidal ones. Their approach is particularly appropriate for studies where accurate evaluation of the vacuum field has been obtained. Ours provides a useful complement because it enables one to understand the contributions of the individual field components to the equilibrium and stability properties of the system.

The introduction of characteristic coordinates may have more general applications. The operator $\mathbf{B} \cdot \nabla$ reduces to a single partial derivative in these coordinates, and this permits integration of the magnetic differential equations which arise in the helical-axis stellarator-expansion formalism. We note that the $\mathbf{B} \cdot \nabla$ operator appears often in MHD calculations, and other representations such as Hamada coordinates which serve to simplify this operator are often

useful. A possible extension of this work would be to apply the stellarator-expansion technique in characteristic coordinates to more complicated vacuum field geometries. This can be done even in the case where analytic expressions are not available for the characteristic coordinates, provided an equation for these coordinates can be integrated numerically. Hender and Carreras[24] have successfully implemented this type of numerical technique in a vacuum flux coordinate system.

In summary, in this paper we have used stellarator-expansion techniques to provide an asymptotic model of stellarators with a helical magnetic axis. We note that the characteristic coordinates necessary to represent the equilibrium solutions properly may have more general uses, since they greatly simplify the $\mathbf{B} \cdot \nabla$ operator. We have used the helical-axis stellarator expansion in connection with an equilibrium computer code to estimate the equilibrium properties of two stellarators. The basic expansion seems useful in this context, and modifications of the basic expansion for the modeling of systems with more complicated vacuum fields should be possible.

Acknowledgments

One of us (AEK) thanks Prof. M. D. Kruskal for many helpful discussions, and for sponsorship under the Program in Applied Mathematics at Princeton University. Additionally, we have both benefited from interaction with colleagues at Princeton and elsewhere. This work was supported by the U. S. Department of Energy under Contract No. DE-AC02-76-CHO-3073.

REFERENCES

[1]L. Spitzer, Jr., Phys. Fluids **1**, 253 (1958).

[2]H. R. Koenig, U.S. Atomic Energy Commission Rept. No. NYO-8054 (PM-S-40, 1959).

[3]J. L. Johnson, Nucl. Technol./Fusion **2**, 340 (1982).

[4]A. H. Boozer, T. K. Chu, R. L. Dewar, H. P. Furth, J. A. Goree, J. L. Johnson, R. M. Kulsrud, D. A. Monticello, G. Kuo-Petravic, G. V. Sheffield, S. Yoshikawa, and O. Betancourt, in *Plasma Physics and Controlled Nuclear Fusion Research* (IAEA, Baltimore, 1982), Vol. 3, p. 129.

[5]J. P. Friedberg, Rev. Mod. Phys. **54**, 801 (1982).

[6]F. Bauer, O. Betancourt, and P. Garabedian, *Magnetohydrodynamic Equilibrium and Stability of Stellarators* (Springer-Verlag, New York, NY 1984).

[7]V. D. Shafranov, Phys. Fluids **26**, 357 (1983).

[8]C. Mercier and H. Luc, *Lectures in Plasma Physics* (Commission of the European Communities, Luxembourg, 1974).

[9]S. Nagao, H. Chishma, and N. Sasaki, J. Phys. Soc. Japan **42**, 1075 (1977).

[10]J. M. Greene and J. L. Johnson, Phys. Fluids **4**, 875 (1961).

[11]G. Anania, J. L. Johnson, and K. E. Weimer, Phys. Fluids **26**, 2210 (1983).

[12]N. Krylov and N. Bogoliubov, *Introduction to Nonlinear Mechanics* (Princeton University Press, Princeton, NJ 1947).

[13]M. D. Kruskal, in *Mathematical Models in Physical Science*, edited by S. Drobot (Prentice-Hall, Inc., Englewood Cliffs, NJ 1963) p. 17.

[14]M. D. Kruskal and R. M. Kulsrud, Phys. Fluids **1**, 265 (1958).

[15]J. L. Johnson, H. E. Dalhed, J. M. Greene, R. C. Grimm, Y. Y. Hsieh, S. C.

Jardin, J. Manickam, M. Okabayashi, R. G. Storer, A. M. M. Todd, D. E. Voss, and K. E. Weimer, J. Comput. Phys. **32**, 212 (1979).

[16]A. E. Koniges, PhD Thesis, Princeton University (1984).

[17]F. B. Hildebrand, *Methods of Applied Mathematics* (Prentice-Hall, Inc., Englewood Cliffs, NJ 1965) p. 306.

[18]S. Nagao, H. Watanabe, Y. Funato, I. Sakamoto, N. Sasaki, and K. Nukui, *Proceedings of the Seventh Symposium on Engineering Problems of Fusion Research* (Knoxville, TN 1977), Vol. 1, p. 841.

[19]S. Nagao and Asperator Group, International Workshop on Stellarators (Schloss Ringberg, F.R.G., 1980) Paper B-3-6.

[20]Y. Funato, I. Sakamoto, T. Takahashi, S. Kitajima, Y. Ikeda, M. Nakazawa, H. Watanabe, S. Nagao, and Asperator group, *Proceeedings of the Tenth European Conference on Controlled Fusion and Plasma Physics* (Moscow, 1981), Vol. 1, p. 365.

[21]Y. Funato, I. Sakamoto, T. Asaishi, T. Saito, and S. Nagao, Plasma Phys. **22**, 545 (1980).

[22]B. A. Trubnikov and A. V. Dobryakov, Sov. J. Plasma Phys. **8**, 29 (1982).

[23]G. Anania and J. L. Johnson, Phys. Fluids **26**, 3070 (1983).

[24]T. C. Hender and B. A. Carreras, Phys. Fluids **27**, 2101 (1984).

TABLE I. *Parameters for the Asperator NP Devices*

Parameter	NP-3	NP-4
Average major radius (R)	80 cm	152.4 cm
Minor radius (a)	3.5 cm	13.3 cm
Bore radius of limiter (a_p)	3.0 cm	9.5 cm
Number of periods (N)	16	8
Helical radius (r_0)	5.0 cm	19.05 cm
$\Delta = r_o/a_p$	1.67	2.01
$\epsilon = a_p/R$	0.038	0.062
$\gamma = \epsilon N$	0.60	0.50

FIGURES

FIG. 1. Model equilibrium configuration of NP-3 for $\langle\beta\rangle = 34\,\%$. (a) Magnetic flux surfaces at $t = 0$, $\pi/2$, and π. (b)ι versus $\Psi_{\rm pol}$. Dashed line is vacuum value. (c) $V'(\Psi_{\rm tor})$ versus $\Psi_{\rm pol}$. Dashed line is vacuum value.

FIG. 2. Effect of pressure variation on the equilibrium properties of NP-3: flux surfaces, rotational transform ι, and $V'(\Psi_{\rm tor})$ with (a) $\langle\beta\rangle = 0\,\%$, (b) $\langle\beta\rangle = 17\,\%$, and (c) $\langle\beta\rangle = 50\,\%$.

FIG. 3. Effect of pressure variation on the equilibrium properties of NP-4 with (a) $\langle\beta\rangle = 0\,\%$, (b) $\langle\beta\rangle = 17\,\%$, and (c) $\langle\beta\rangle = 49\,\%$.

FIG. 4. Equilibrium properties for NP-4 using different pressure function exponents: (a) $k = 1.5$ and (b) $k = 3.0$. The corresponding pressure function P and the parallel current distribution σ are also shown for each case.

#84T0236

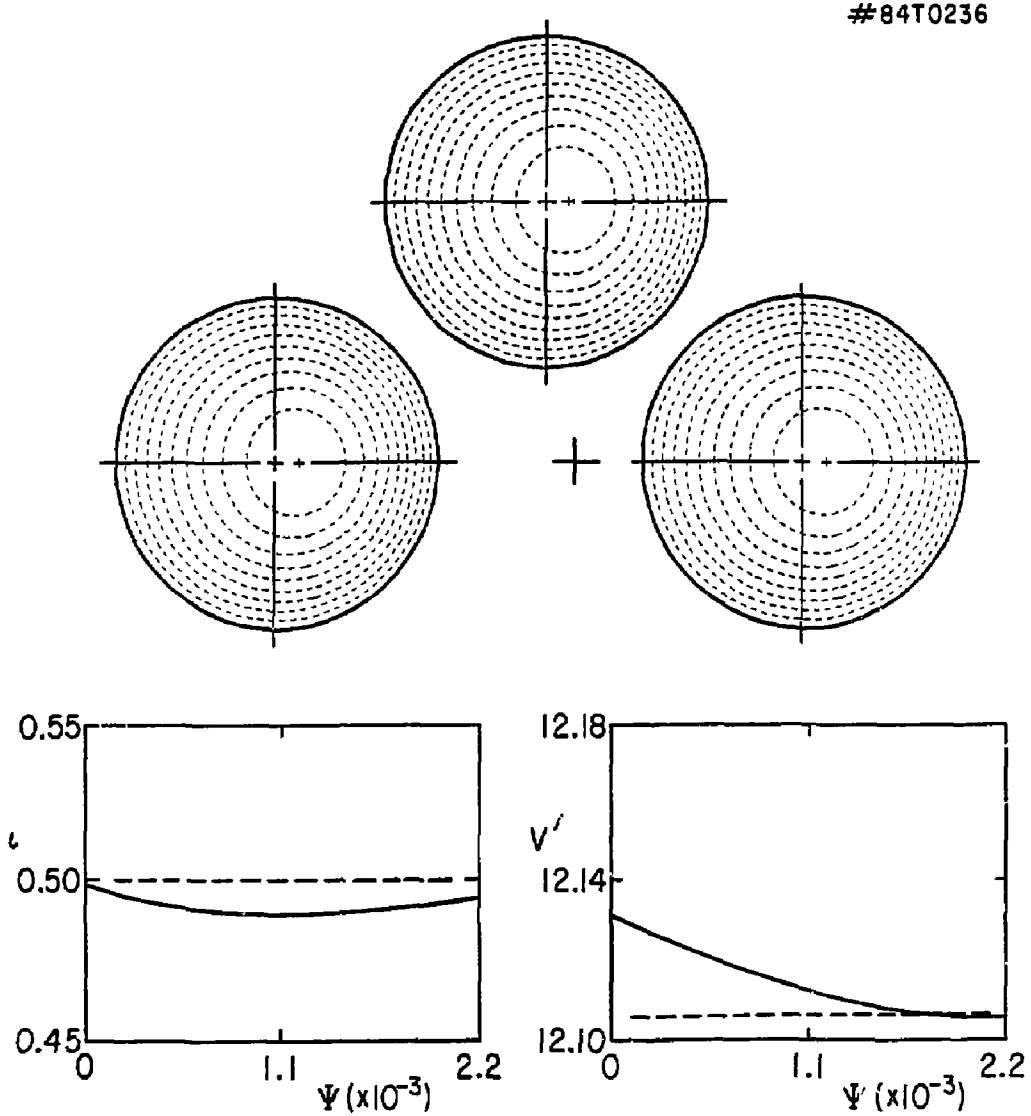

Fig. 1

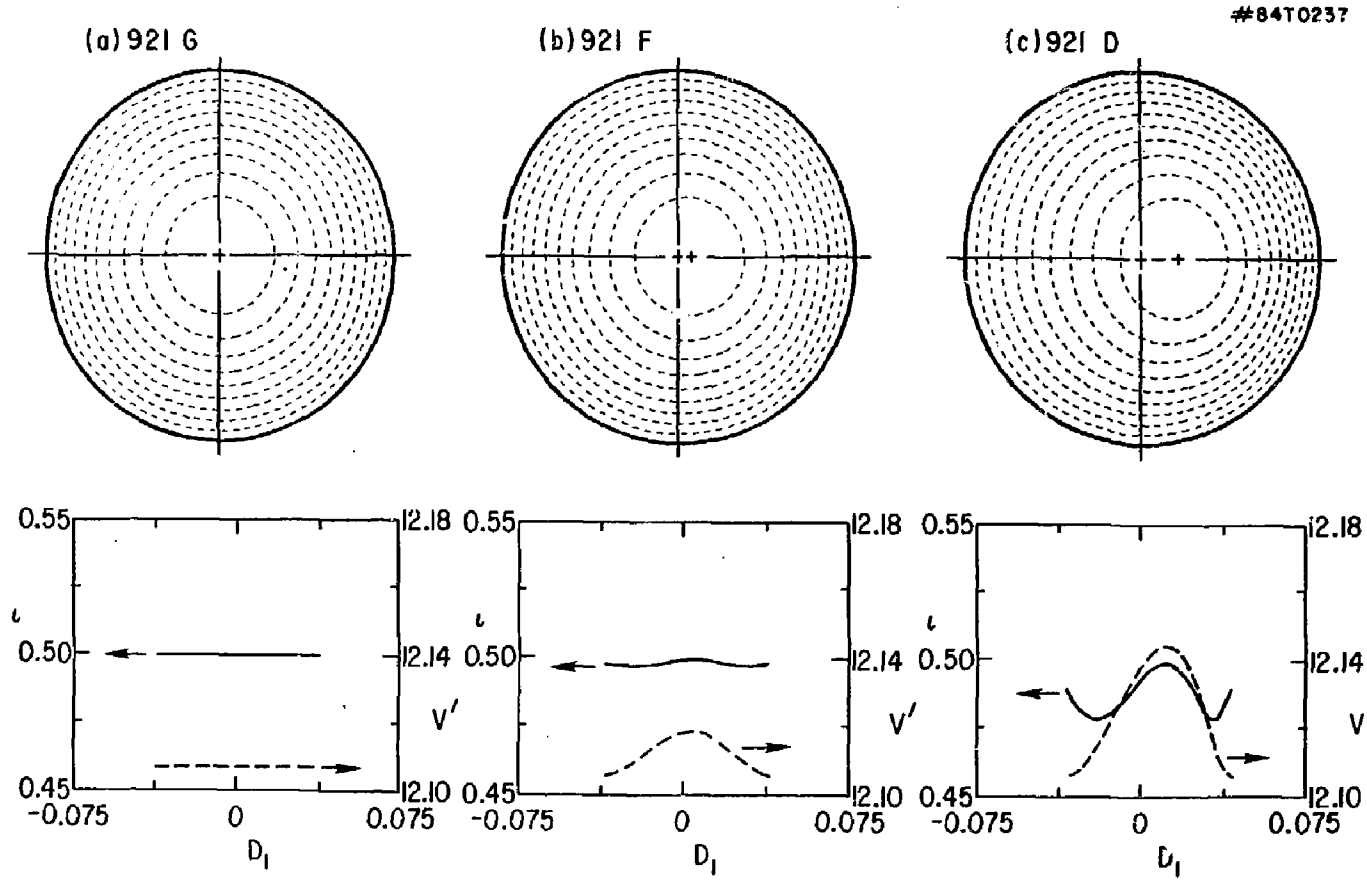
#84T0237
(a) 921 G
(b) 921 F
(c) 921 D
0.55
0.50
0.45
ι
12.18
12.14
12.10
V′
-0.075
0
0.075
D1

Fig. 2

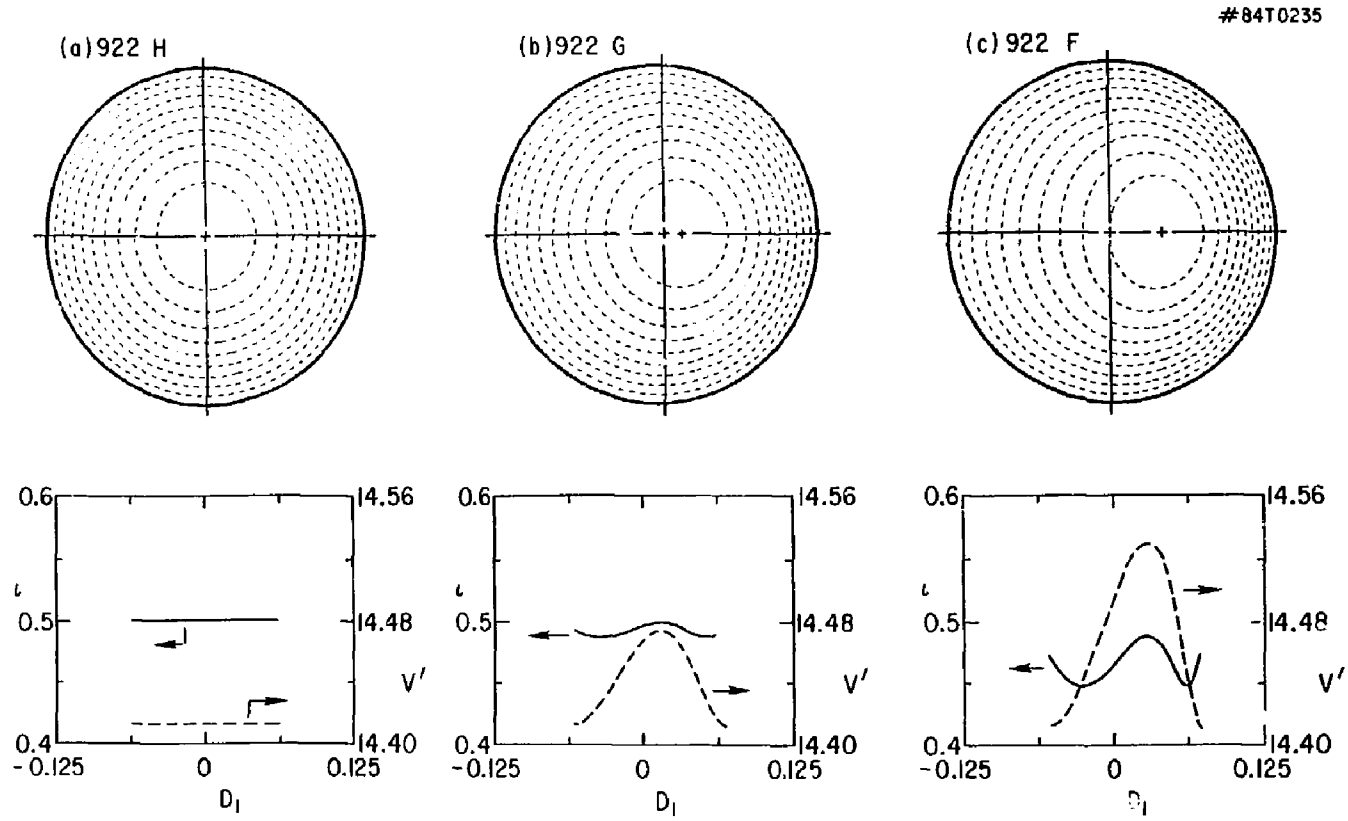
#84T0235
(a)922 H
(b)922 G
(c)922 F
0.6
0.5
0.4
14.56
14.48
14.40
V'
ι
-0.125
0
0.125
D_I

Fig. 3

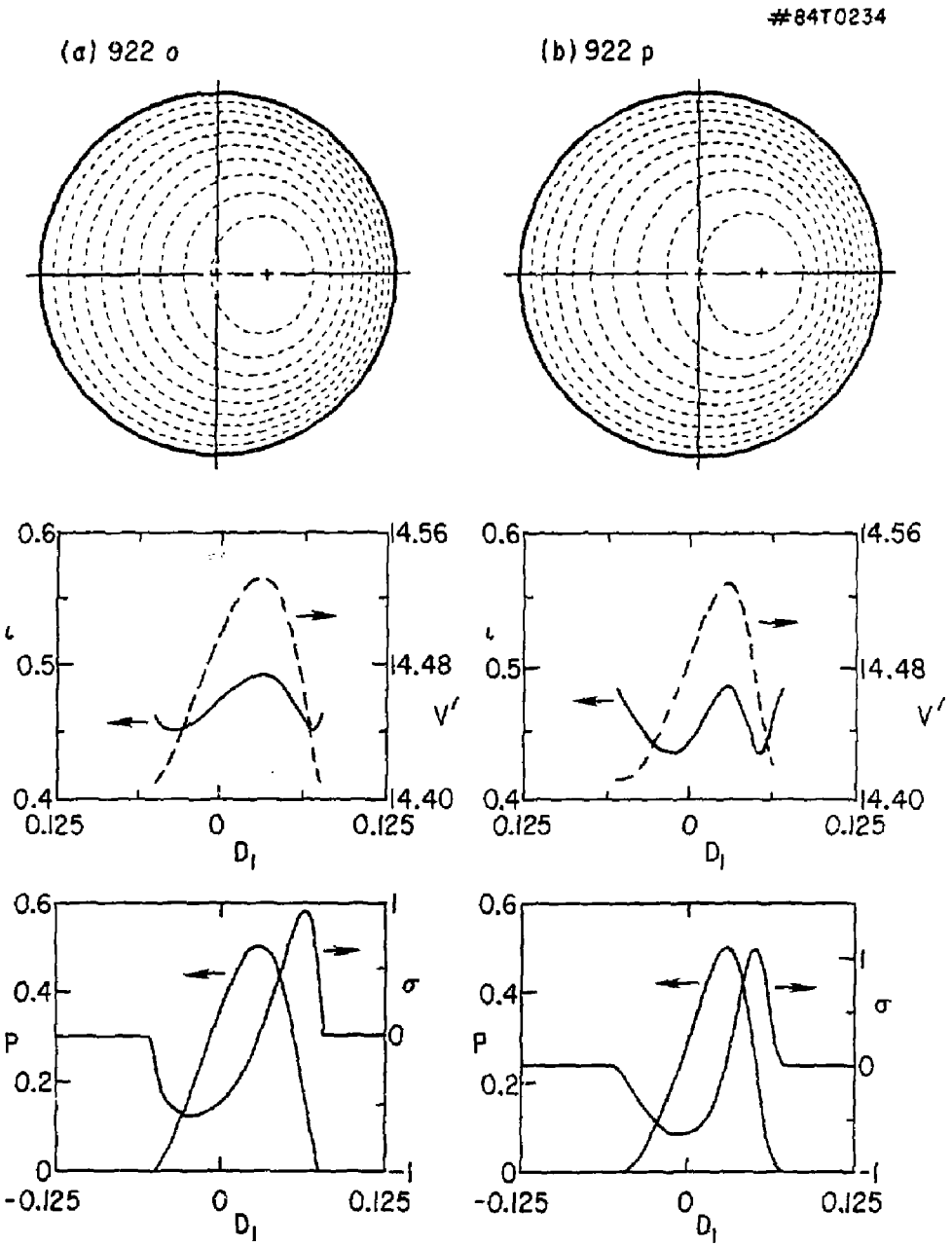
#84T0234
(a) 922 o
(b) 922 p
0.6
0.5
0.4
ι
14.56
14.48
14.40
V′
0.125
0
0.125
D_I
0.6
0.4
0.2
0
P
1
0
-1
σ
-0.125
0
0.125
D_I

Fig. 4

REPRODUCED FROM
BEST AVAILABLE COPY

EXTERNAL DISTRIBUTION IN ADDITION TO UC-20

Plasma Res Lab, Austra Nat'l Univ, AUSTRALIA
Dr. Frank J. Paoloni, Univ of Wollongong, AUSTRALIA
Prof. I.R. Jones, Flinders Univ., AUSTRALIA
Prof. M.H. Brennan, Univ Sydney, AUSTRALIA
Prof. F. Cap, Inst Theo Phys, AUSTRIA
Prof. Frank Verheest, Inst theoretische, BELGIUM
Dr. D. Palumbo, Dg XII Fusion Prog, BELGIUM
Ecole Royale Militaire, Lab de Phys Plasmas, BELGIUM
Dr. P.H. Sakanaka, Univ Estadual, BRAZIL
Dr. C.R. James, Univ of Alberta, CANADA
Prof. J. Teichmann, Univ of Montreal, CANADA
Dr. H.M. Skarsgard, Univ of Saskatchewan, CANADA
Prof. S.R. Sreenivasan, University of Calgary, CANADA
Prof. Tudor W. Johnston, INRS-Energie, CANADA
Dr. Hannes Barnard, Univ British Columbia, CANADA
Dr. M.P. Bachynski, MPB Technologies, Inc., CANADA
Chalk River, Nucl Lab, CANADA
Zhenowu Li, SW Inst Physics, CHINA
Library, Tsing Hua University, CHINA
Librarian, Institute of Physics, CHINA
Inst Plasma Phys, Academia Sinica, CHINA
Dr. Peter Lukac, Komenskeho Univ, CZECHOSLOVAKIA
The Librarian, Culham Laboratory, ENGLAND
Prof. Schatzman, Observatoire de Nice, FRANCE
J. Radet, CEN-BP6, FRANCE
AM Dupas Library, AM Dupas Library, FRANCE
Dr. Tom Mual, Academy Bibliographic, HONG KONG
Preprint Library, Cent Res Inst Phys, HUNGARY
Dr. S.K. Trehan, Panjab University, INDIA
Dr. Indra Mohan Lal Das, Banaras Hindu Univ, INDIA
Dr. L.K. Chavda, South Gujarat Univ, INDIA
Dr. R.K. Chhajlani, Vikram Univ. INDIA
Dr. B. Dasgupta, Saha Inst, INDIA
Dr. P. Kaw, Physical Research Lab, INDIA
Dr. Phillip Rosenau, Israel Inst Tech, ISRAEL
Prof. S. Cuperman, Tel Aviv University, ISRAEL
Prof. G. Rostagni, Univ Di Padova, ITALY
Librarian, Int'l Ctr Theo Phys, ITALY
Miss Clelia De Palo, Assoc EURATOM-ENEA, ITALY
Biblioteca, del CNR EURATOM, ITALY
Dr. H. Yamato, Toshiba Res & Dev, JAPAN
Direc. Dept. Lg. Tokamak Dev. JAERI, JAPAN
Prof. Nobuyuki Inoue, University of Tokyo, JAPAN
Research Info Center, Nagoya University, JAPAN
Prof. Kyoji Nishikawa, Univ of Hiroshima, JAPAN
Prof. Sigeru Mori, JAERI, JAPAN
Library, Kyoto University, JAPAN
Prof. Ichiro Kawakami, Nihon Univ, JAPAN
Prof. Satoshi Itoh, Kyushu University, JAPAN
Dr. D.I. Choi, Adv. Inst Sci & Tech, KOREA
Tech Info Division, KAERI, KOREA
Bibliotheek, Fom-Inst Voor Plasma, NETHERLANDS
Prof. B.S. Liley, University of Waikato, NEW ZEALAND
Prof. J.A.C. Cabral, Inst Superior Tecn, PORTUGAL
Dr. Octavian Petrus, ALI CUZA University, ROMANIA
Prof. M.A. Hellberg, University of Natal, SO AFRICA
Dr. Johan de Villiers, Plasma Physics, Nucor, SO AFRICA
Fusion Div. Library, JEN, SPAIN
Prof. Hans Wilhelmson, Chalmers Univ Tech, SWEDEN
Dr. Lennart Stenflo, University of UMEA, SWEDEN
Library, Royal Inst Tech, SWEDEN
Centre de Recherchesen, Ecole Polytech Fed, SWITZERLAND
Dr. V.T. Tolok, Kharkov Phys Tech Ins, USSR
Dr. D.D. Ryutov, Siberian Acad Sci, USSR
Dr. G.A. Eliseev, Kurchatov Institute, USSR
Dr. V.A. Glukhikh, Inst Electro-Physical, USSR
Institute Gen. Physics, USSR
Prof. T.J.M. Boyd, Univ College N Wales, WALES
Dr. K. Schindler, Ruhr Universitat, W. GERMANY
Nuclear Res Estab, Julich Ltd, W. GERMANY
Librarian, Max-Planck Institut, W. GERMANY
Bibliothek, Inst Plasmaforschung, W. GERMANY
Prof. R.K. Janev, Inst Phys, YUGOSLAVIA